

589 nm Light Source Based on Raman Fiber Laser

Yan FENG*, Shenghong HUANG, Akira SHIRAKAWA and Ken-Ichi UEDA

Institute for Laser Science, University of Electro-Communications, 1-5-1 Chofugaoka, Chofu, Tokyo 182-8585, Japan

(Received January 7, 2004; accepted April 1, 2004; published May 21, 2004)

A fiber-based continuous-wave laser at 589 nm was demonstrated by intracavity frequency doubling of a Raman fiber laser at 1178 nm in a type-I noncritically phase matched lithium triborate crystal. The yellow laser output was limited by the emergence of higher order Stokes Raman emission and the broad linewidth of the fundamental laser at 1178 nm.

[DOI: 10.1143/JJAP.43.L722]

KEYWORDS: Raman fiber laser, intracavity frequency doubling, lithium triborate, laser guided star, sodium D₂ line, stimulated Raman scattering

Harmonic generation using nonlinear optical crystals is currently the most efficient approach of obtaining visible and ultraviolet lasers. Diode-pumped Nd-doped solid-state lasers can operate in the blue, green, and red spectral regions by intracavity frequency doubling. However, there are few solid-state laser sources that can efficiently produce laser emission in a region covering 550 to 650 nm for the absence of fundamental lasers that can operate efficiently there. Laser sources in yellow-orange spectra are of interest for many applications in metrology, remote sensing, and medicine.¹⁾ Several approaches have been used to generate all-solid-state sources in yellow-orange wavelength region: solid dye lasers,²⁾ frequency doubling of crystal Raman lasers³⁾ or LiF:F₂⁻ lasers,⁴⁾ and sum-frequency mixing of two Nd laser lines at 1064 nm and 1319 nm.^{5,6)} The most impressive study to date is on a 20 W continuous wave (CW) laser at 589.159 nm by sum-frequency mixing two injection-locked Nd:YAG lasers in lithium triborate (LBO) in a doubly resonant external cavity.⁵⁾ This study was aimed at building a laser source for sodium D₂ laser guided star for adaptive optical systems,⁶⁻⁸⁾ where high-duty-cycle sources such as CW are preferred to avoid saturation.⁹⁾ However, the entire system was very complex and expensive.

Our approach is to generate a 589 nm laser source by frequency doubling of a Raman fiber laser at 1178 nm. Fiber lasers are easy to handle and excellent beam quality can be achieved with single-mode fibers. Moreover, CW Raman fiber laser in a broad wavelength range can be generated despite the low Raman gain in glass, because of the large interaction length available in fibers. These characteristics make Raman fiber lasers potentially attractive CW laser sources for sodium laser-guided star systems. A laser at 1178 nm by stimulated Raman scattering in phosphosilicate single-mode fibers has already been investigated.¹⁰⁾ In this letter, yellow emission at 589 nm by intracavity frequency doubling of a Raman fiber laser emitting at 1178 nm is described.

A sketch of the experimental setup is shown in Fig. 1. An ytterbium-doped double-clad fiber laser emitting at 1100 nm was used as the pump source. The pump source fiber end was spliced to a fiber Bragg grating (FBG) (reflectivity > 99% at 1178 nm and bandwidth of 1.2 nm). Since both the pump fiber and the FBG are made of Flexcor-1060 fiber, a very low loss splicing was achieved between them. The Raman gain fiber was a 300-m-long phosphorous-doped

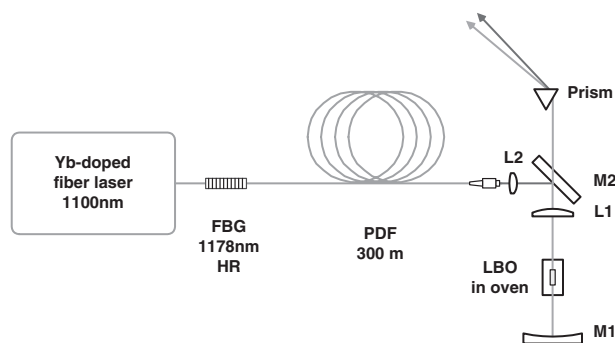


Fig. 1. Schematic of the experimental setup.

single-mode optical fiber (PDF), which had 12 mol % of P₂O₅ and a refractive index difference between the core and clad of 0.0107. A small mismatch in the mode field diameters of the PDF and Flexcor-1060 fiber resulted in a splicing loss of only about 0.2 dB between them. Aspheric lens L2 (focal length: 8 mm) was used to collimate the Raman laser. The beam was focused once again into LBO crystal using lens L1 (focal length: 50 mm). Both lenses were coated with antireflection coating for 1178 nm. Frequency doubling was achieved in a type-I noncritically phase-matched LBO crystal (3 × 3 × 20 mm³) mounted in an oven with temperature control. Concave mirror M1 (50 mm radius of curvature and HR at around 1178 nm) was used as the end-mirror. Dichroic mirror M2 (highly reflecting at 1178 nm and transmitting at 589 nm) was used as the output coupler for 589 nm. The visible light escaping from the cavity through M2 was separated from infrared radiation leaking through M2 by a Brewster prism. Spectra of the output were measured with an AQ-6315A optical spectrum analyzer (ANDO Co.) directly after dichroic mirror M2.

The Raman spectrum of the PDF contains two peaks: one at 1330 cm⁻¹ is sharp and corresponds to the vibration mode of double-bonded oxygen with phosphor atoms and the other at 490 cm⁻¹ is broader and corresponds to the vibration of oxygen with silicon atoms.¹⁰⁾ A 602 cm⁻¹ Raman shift is required to convert the pump laser of 1100 nm to 1178 nm laser emission. The Raman gain at around 602 cm⁻¹ is not the peak value but a high-efficiency Raman laser has been demonstrated with such a configuration.¹⁰⁾

Intracavity doubling was used to increase the efficiency of second harmonic generation (SHG). However, one will see in the following paragraphs that this approach gives rise to other difficulties. The LBO crystal was cut at $\theta = 90^\circ$ and

*E-mail address: feng@ils.uec.ac.jp

$\phi = 0^\circ$. Calculated by SNLO, a type-I noncritical phase matching condition can be realized near 313 K with effective nonlinear coefficient $d_{\text{eff}} = 8.39 \times 10^{-1}$ pm/V and good tolerance in temperature, bandwidth, and acceptance angle. The advantages of noncritical phase matching are the absence of laser beam walk-off, so one can use a long crystal to obtain higher conversion efficiency and the absence of the degradation of the beam quality. The beam was focused near the middle of the LBO crystal; the beam waist was measured and found to be about 40 μm , which was smaller than the optimum value of 57 μm for a 20-mm-long nonlinear crystal and 1178 nm fundamental wavelength according to Boyd and Kleinman.¹¹⁾ However, according to their theory, the focusing parameter is not very critical; it is expected that the efficiency is within 10% of that for optimum focusing.

In our experiments, we first aligned the optics without the LBO crystal. Once the cavity was optimized for the 1178 nm fundamental wavelength, the crystal was inserted at the beam waist, taking into account the refraction in the crystal. Then, because of the light refraction in the crystal, reflective mirror M1 had to be moved farther from the crystal to fulfill the condition for a stable cavity. The upconverted visible light was reflected by M1, and escaped from the cavity through M2.

A laser threshold as low as 1.8 W was obtained. After optimizing the alignment of optical components at a certain pump power, we measured the 589 nm output as a function of pump power without changing the alignment. Figure 2 shows two curves measured after different alignments. Curve No. 1 is the one that was optimized for the yellow output at low pump power (5.6 W), whereas curve No. 2 was optimized for high pump power (11 W). This dependence on the optimizing point may result from some thermally induced light path deviation inside the cavity. Notably, heating at the fiber end was not trivial due to the not-100% coupling from a free space to the fiber. When the fiber end was heated, the local refractive index changed and then the light beam deviated. Because heat increased when the pump power increased, the light path depended on the pump power. This can explain why the optimum alignment for a different pump power is different. Just above the threshold, the output at 589 nm increased nonlinearly with pump power, because of the square law dependence of conversion efficiency on fundamental laser intensity, but was soon saturated. The maximum output at 589 nm was about 10 mW.

The saturation of the output was due to the emergence of higher order Stokes Raman lasers. Figure 3 shows the emission spectra detected directly after dichroic mirror M2. (a) and (b) were taken at pump powers of 5.6 W and 11 W, respectively, in an alignment corresponding to curve No. 1 in Fig. 2. The emission at 1250.5 nm corresponds to the Stokes shift from 1178 nm by 490 cm^{-1} , the first peak of Raman gain. After the threshold of 1250.5 nm emission is achieved, intracavity power at 1178 nm no longer increases. Such a behavior was also observed in experiments on fundamental lasers.¹⁰⁾

Figure 4 shows a typical spectrum of the visible output. Interestingly, one can find, besides the stronger emission at 589 nm, lines at 550 nm, 569 nm, 606.5 nm, and 625 nm,

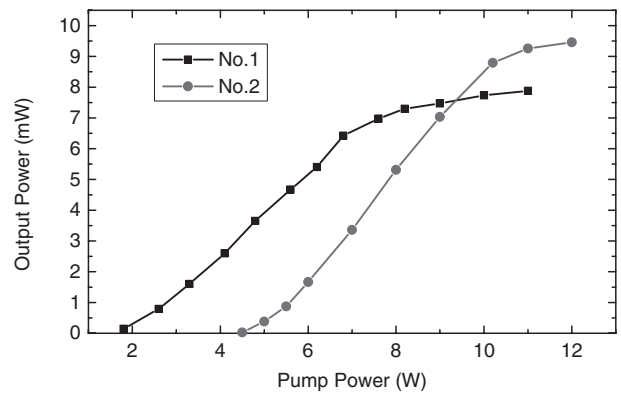


Fig. 2. 589 nm laser output versus pump power, measured at two different alignments. Curve No. 1 was optimized for the yellow output at low pump power (5.6 W), whereas curve No. 2 was optimized for high pump power (11 W).

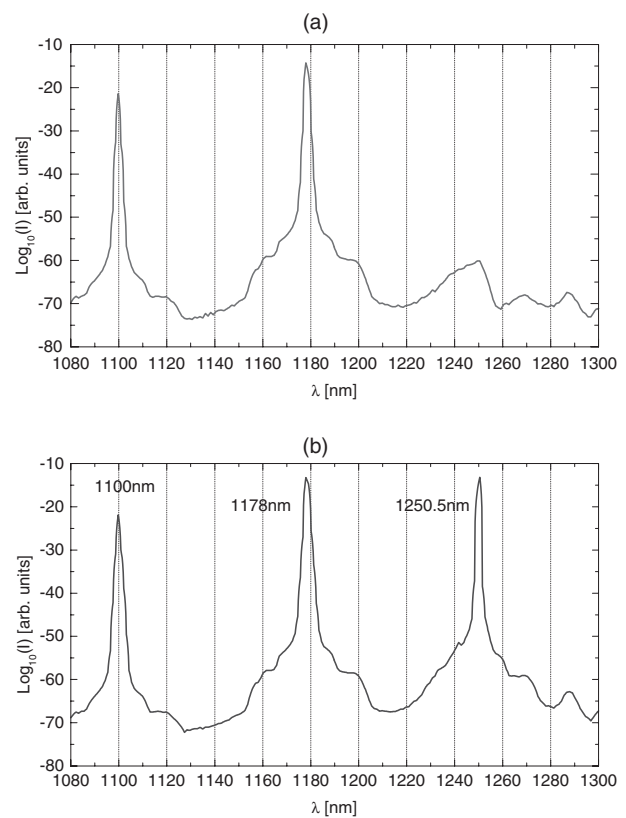


Fig. 3. Emission spectra detected directly after bichromatic mirror M2. (a) and (b) were taken at pump powers of 5.6 W and 11 W, respectively, in an alignment corresponding to curve No. 1 in Fig. 2.

which correspond to frequency mixing of 1100 nm + 1100 nm, 1100 nm + 1178 nm, 1178 nm + 1250.5 nm, and 1250.5 nm + 1250.5 nm, respectively. Because these frequency-mixing channels are out of phase-matching condition, conversion efficiencies are low. We also observed brighter emissions at 569 nm and 606.5 nm when the crystal temperature was tuned to the phase matching temperatures of about 70°C and 20°C, respectively.

Both 1178 nm and 589 nm emission spectra were broadened as the pump power increased due to the broad Raman spectrum and high intracavity power. At the saturation stage, typical linewidths were 2 nm and 0.7 nm, respectively.

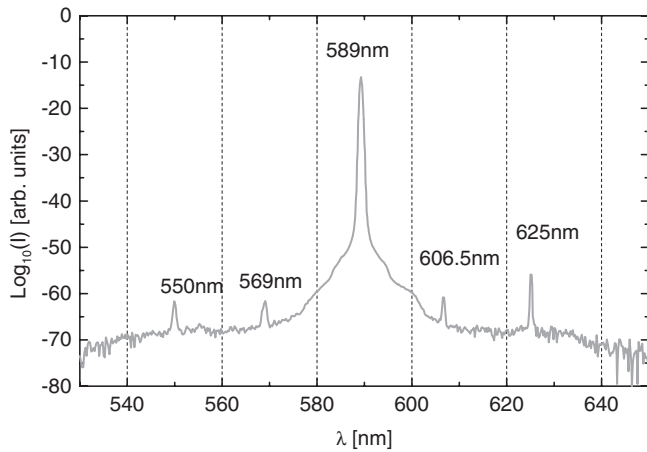


Fig. 4. Emission spectrum of the visible output detected directly after bichromatic M2.

It is noteworthy that in our experiments, conversion efficiency was very low, since only a 10 mW level was achieved from the multiwatt pumping power. There are many factors contributing to this low efficiency. The first factor is the emergence of higher order Stokes Raman emission in the fiber. This could be eliminated by tailoring the optics, by adjusting the spectrum of the optical components, and by adjusting the fiber length. In these experiments, standard commercially available optical components were used. The second factor is the broad bandwidth of the Raman fiber laser, which influences the frequency-doubling efficiency greatly. Another limitation is the random polarization of the Raman fiber laser, so only half of the power is useful. Adding polarizing elements into the system may solve this. In a word, one should try to improve the conversion process from 1100 nm to 1178 nm and from 1178 nm to 589 nm, while at the same time suppressing other competing processes.

The broad spectrum of the Raman gain gives the flexibility on laser wavelength, so the visible laser is feasible

over a wide spectral range. However, the drawback is the difficulty to achieve a narrow bandwidth laser. In this work, emission at 589 nm with a linewidth of 0.7 nm was generated, which is too broad for some important applications. For example, a sodium laser-guided star system requires lasers with bandwidths of about 100–500 MHz (0.5–2.5 pm). Our future work is to find solutions or other approaches of decreasing the linewidth of the laser output and increasing the efficiency as well.

In summary, we have demonstrated for the first time to our knowledge a fiber-based CW laser at 589 nm by intracavity frequency doubling of a Raman fiber laser at 1178 nm with a type-I noncritically phase-matched lithium triborate crystal. A maximum output of 10 mW was obtained. The emergence of higher-order Stokes Raman emission and the broad linewidth of the 1178 nm laser prevented us from obtaining higher conversion efficiency. Frequency-sum mixing of Raman emissions and that between the pump beam and signal were also observed.

This work is supported by the 21st Century COE program of the Ministry of Education, Culture, Sports, Science and Technology of Japan. Yan Feng thanks J.F. Bisson for reading the manuscript.

- 1) H. M. Kretschmann, F. Heine, G. Huber and T. Halldorsson: *Opt. Lett.* **22** (1997) 1461.
- 2) H. Watanabe, T. Omatsu and M. Tateda: *Opt. Express* **11** (2003) 176.
- 3) H. M. Pask and J. A. Piper: *Opt. Lett.* **24** (1999) 1490.
- 4) S. M. Giffin, G. W. Baxter, L. T. McKinnie and V. V. Ter-Mikirtychev: *Appl. Opt.* **41** (2002) 4331.
- 5) J. C. Bienfang, C. A. Denman, B. W. Grime, P. D. Hillman, G. T. Moore and J. M. Telle: *Opt. Lett.* **28** (2003) 2219.
- 6) J. D. Vance, C. Y. She and H. Moosmuller: *Appl. Opt.* **37** (1998) 4891.
- 7) H. Moosmuller and J. D. Vance: *Opt. Lett.* **22** (1997) 1135.
- 8) J.-P. Pique and S. Farinotti: *J. Opt. Soc. Am. B* **20** (2003) 2093.
- 9) P. W. Milonni, H. Fearn, J. M. Telle and R. Q. Fugate: *J. Opt. Soc. Am. A* **16** (1999) 2555.
- 10) S. Huang, Y. Feng, A. Shirakawa and K. Ueda: *Jpn. J. Appl. Phys.* **42** (2003) L 1439.
- 11) G. D. Boyd and D. A. Kleinman: *J. Appl. Phys.* **39** (1968) 3597.